APPENDICES

APPENDIX A

The Joint Committee for Powder Diffraction Standards (JCPDS) used for the present research [81]

1. Cu_3BiS_3, JCPDS file number 43-1479

Name and formula

Reference code:	43-1479
Mineral name:	Wittichenite
Common name:	klaprothite
PDF index name:	Copper Bismuth Sulfide
Empirical formula:	$BiCu_3S_3$
Chemical formula:	Cu_3BiS_3

Crystallographic parameters

Crystal system:	Orthorhombic		
Space group:	$P2_12_12_1$	Alpha (degree):	90.0000
Space group number:	19	Beta (degree):	90.0000
a (Å):	7.6960	Gamma (degree):	90.0000
b (Å):	10.3880	Volume of cell:	536.59
c (Å):	6.7119	Z:	4.00

Subfiles and Quality

Subfiles:	Inorganic, Mineral, Alloy, metal or intermetalic Corrosion
Quality:	Star (S)

Comments

Color:	Light gray metallic
General comments:	(*) Department of Geology and Geophysics, University of Calgary, Alberta, Canada.
Sample source:	Specimen from Wittichen, Schwarzwald, Baden-Wuerttemberg, Germany (Glenbow Museum, Calgary GA382).
Structure:	Skinnerite is the Sb analogue.
Analysis:	X-ray emission analysis under SEM: major Cu, Bi and S.
Additional pattern:	To replace 9-488. See ICSD 14305 (PDF 71-2115).

References

Primary reference:	Cleveland, P., McCarthy, G., *Bayliss, P., North Dakota State University, Fargo, North Dakota, USA., *ICDD Grant-in-Aid*, (1991)
Unit cell:	Kocman, V., Nuffield, E., Acta Crystallogr., *Sec. B*, **29**, 2528, (1973)

Stick Pattern

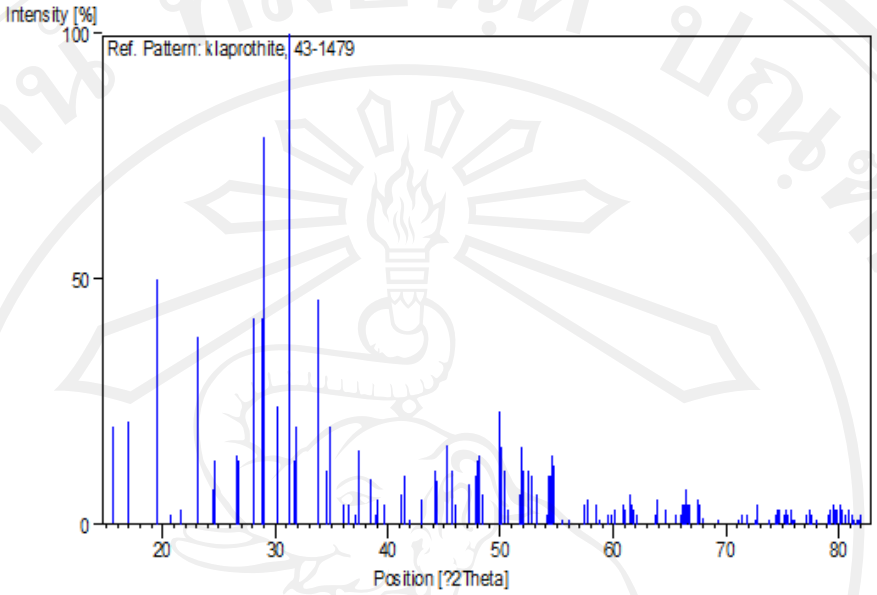

Peak list

No.	h	k	l	d [A]	I [%]
1	0	1	1	5.63900	20.0
2	0	2	0	5.19300	21.0
3	1	1	1	4.54800	50.0
4	1	2	0	4.30100	2.0
5	0	2	1	4.11100	3.0
6	2	0	0	3.84800	38.0
7	1	2	1	3.62700	7.0
8	2	1	0	3.61000	13.0
9	0	0	2	3.35500	14.0
10	2	0	1	3.33900	13.0
11	2	1	1	3.17800	42.0
12	2	2	0	3.09200	42.0

No.	h	k	l	d [A]	I [%]
13	0	3	1	3.07700	79.0
14	1	1	2	2.95000	24.0
15	1	3	1	2.85800	100.0
16	0	2	2	2.81700	13.0
17	2	2	1	2.80800	20.0
18	1	2	2	2.64700	46.0
19	0	4	0	2.59700	11.0
20	2	3	0	2.57500	20.0
21	3	1	0	2.49170	4.0
22	1	4	0	2.45920	4.0
23	0	4	1	2.42140	2.0
24	2	3	1	2.40210	14.0
25	3	0	1	2.39610	15.0
26	3	1	1	2.33560	9.0
27	1	4	1	2.31100	2.0
28	3	2	0	2.30050	5.0
29	2	2	2	2.27350	4.0
30	0	1	3	2.18670	6.0
31	3	2	1	2.17610	10.0
32	2	4	0	2.15340	1.0
33	1	1	3	2.10380	5.0
34	2	4	1	2.04950	11.0
35	2	3	2	2.04300	9.0

No.	h	k	l	d [A]	I [%]
36	3	0	2	2.03890	8.0
37	3	1	2	1.99970	16.0
38	1	2	3	1.98470	11.0
39	3	3	1	1.97040	4.0
40	1	5	1	1.92130	8.0
41	2	1	3	1.90140	10.0
42	3	2	2	1.89740	13.0
43	4	1	0	1.89190	14.0
44	0	3	3	1.87920	6.0
45	1	3	3	1.82540	23.0
46	4	1	1	1.82100	16.0
47	2	2	3	1.81200	11.0
48	4	2	0	1.80370	3.0
49	0	5	2	1.76660	6.0
50	2	5	1	1.76350	16.0
51	3	4	1	1.76030	16.0
52	3	3	2	1.75650	11.0
53	4	2	1	1.74210	11.0
54	0	6	0	1.73140	10.0
55	1	5	2	1.72150	6.0
56	0	4	3	1.69530	2.0
57	2	3	3	1.68790	10.0
58	3	0	3	1.68560	10.0

No.	h	k	l	d [A]	I [%]
59	4	3	0	1.68160	14.0
60	0	0	4	1.67750	12.0
61	0	1	4	1.65630	1.0
62	1	6	1	1.63810	1.0
63	3	2	3	1.60350	4.0
64	0	2	4	1.59670	5.0
65	2	6	0	1.57890	4.0
66	3	5	1	1.57010	1.0
67	2	4	3	1.55110	2.0
68	4	4	0	1.54550	2.0
69	2	0	4	1.53780	3.0
70	0	5	3	1.52190	4.0
71	3	3	3	1.51610	3.0
72	1	6	2	1.50850	6.0
73	4	3	2	1.50280	4.0
74	5	0	1	1.50060	3.0
75	1	5	3	1.49370	2.0
76	4	0	3	1.45840	2.0
77	3	5	2	1.45490	5.0
78	5	2	1	1.44150	3.0
79	1	7	1	1.42440	2.0
80	2	5	3	1.41600	2.0
81	4	5	0	1.41220	4.0

No.	h	k	l	d [A]	I [%]
82	0	4	4	1.40920	4.0
83	2	3	4	1.40520	7.0
84	4	4	2	1.40370	4.0
85	5	0	2	1.39900	4.0
86	5	1	2	1.38630	5.0
87	2	7	0	1.38480	4.0
88	5	3	1	1.37700	1.0
89	2	7	1	1.35590	1.0
90	2	4	4	1.32340	1.0
91	3	6	2	1.31920	2.0
92	1	1	5	1.31180	2.0
93	3	3	4	1.30120	1.0
94	5	4	1	1.29910	3.0
95	5	3	2	1.29750	4.0
96	6	0	0	1.28260	1.0
97	6	1	0	1.27330	2.0
98	4	4	3	1.27190	3.0
99	5	0	3	1.26820	3.0
100	4	6	1	1.26380	2.0
101	3	7	1	1.26190	2.0
102	6	0	1	1.2600	3.0
103	5	1	3	1.25860	2.0
104	4	1	4	1.25540	3.0

No.	h	k	l	d [A]	I [%]
105	0	3	5	1.25210	1.0
106	6	1	1	1.25070	1.0
107	5	5	0	1.23660	1.0
108	1	3	5	1.23510	2.0
109	5	2	3	1.23160	3.0
110	2	8	0	1.23010	2.0
111	4	2	4	1.22880	2.0
112	6	2	1	1.22400	1.0
113	2	8	1	1.21010	2.0
114	3	6	3	1.20800	3.0
115	0	6	4	1.20460	4.0
116	6	3	0	1.20310	4.0
117	4	6	2	1.20170	3.0
118	3	7	2	1.19940	3.0
119	1	8	2	1.19630	4.0
120	4	5	3	1.19390	3.0
121	1	6	4	1.19030	2.0
122	4	3	4	1.18780	3.0
123	6	3	1	1.18380	2.0
124	3	1	5	1.18210	1.0
125	1	4	5	1.17840	1.0
126	2	7	3	1.17720	1.0
127	4	7	0	1.17550	2.0

2. Cu_3SbS_4, JCPDS file number 10-0472

Name and formula

Reference code:	10-0472
Mineral name:	Famatinite, syn
PDF index name:	Copper Antimony Sulfide
Empirical formula:	Cu_3S_4Sb
Chemical formula:	Cu_3SbS_4

Crystallographic parameters

Crystal system:	Tetragonal	Alpha (?):	90.0000
Space group:	$I\bar{4}2m$	Beta (?):	90.0000
Space group number:	121	Gamma (?):	90.0000
a (?):	5.3800	Calculated density:	4.70
b (?):	5.3800	Measured density:	4.64
c (?):	10.7600	Volume of cell:	311.44
		Z:	2.00

Status, subfiles and quality

Status:	Marked as deleted by ICDD
Subfiles:	Inorganic
	Mineral
	Alloy, metal or intermetalic
Quality:	Blank (B)

Comments

Color: Dark pinkish brown

Sample source: Specimen from Famatina, Argentina.

Additional diffraction line(s): Plus 14 lines to 0.7768.

References

Primary reference: Gaines., *Am. Mineral.*, **42**, 772, (1957)

Stick Pattern

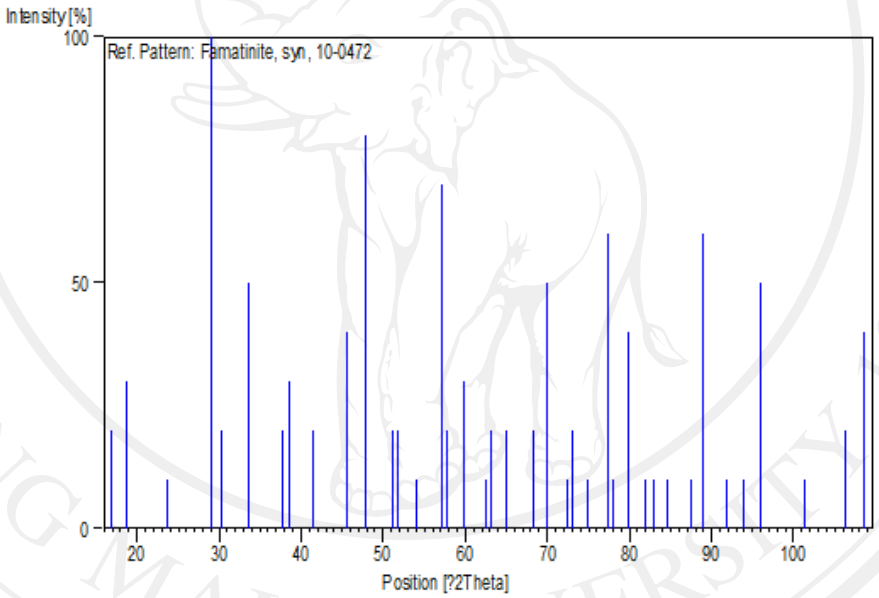

Peak list

No.	h	k	l	d [A]	I [%]
1	0	0	2	5.26000	20.0
2	1	0	1	4.73000	30.0
3	1	1	0	3.75200	10.0
4	1	1	2	3.07100	100.0
5	1	0	3	2.95200	20.0

No.	h	k	l	d [A]	I [%]
6	0	0	4	2.66400	50.0
7	2	0	2	2.39000	20.0
8	2	1	1	2.33600	30.0
9	1	1	4	2.18100	20.0
10	1	0	5	1.98500	40.0
11	2	0	4	1.89500	80.0
12	0	0	6	1.78700	20.0
13	3	0	1	1.76300	20.0
14	3	1	0	1.69300	10.0
15	1	1	6	1.61400	70.0
16	2	1	5	1.59700	20.0
17	2	2	4	1.54700	30.0
18	1	0	7	1.48500	10.0
19	3	2	1	1.46900	20.0
20	3	1	4	1.43400	20.0
21	3	0	5	1.37300	20.0
22	0	0	8	1.34200	50.0
23	2	2	6	1.30400	10.0
24	2	1	7	1.29400	20.0
25	1	1	8	1.26600	10.0
26	3	1	6	1.23200	60.0
27	3	2	5	1.22500	10.0
28	2	0	8	1.20000	40.0

No.	h	k	l	d [A]	I [%]
29	4	2	2	1.17400	10.0
30	1	0	9	1.16400	10.0
31	3	3	4	1.14500	10.0
32	4	1	5	1.11400	10.0
33	2	2	8	1.09900	60.0
34	2	1	9	1.07200	10.0
35	3	1	8	1.05500	10.0
36	1	1	10	1.03700	50.0
37	3	0	9	0.99600	10.0
38	1	0	11	0.96280	20.0
39	4	0	8	0.94910	40.0

3. $CuFeS_2$, JCPDS file number

Name and formula

Reference code:	01-0842
Mineral name:	Chalcopyrite
PDF index name:	Copper Iron Sulfide
Empirical formula:	$CuFeS_2$
Chemical formula:	$CuFeS_2$

Crystallographic parameters

Crystal system:	Tetragonal	Alpha (degre):	90.0000
Space group:	$I\bar{4}2d$	Beta (degree):	90.0000
Space group number:	122	Gamma (degree):	90.0000
a (Å):	5.2400	Measured density:	4.28
b (Å):	5.2400	Volume of cell:	282.81
c (Å):	10.3000	Z:	4.00

Status, subfiles and quality

Status:	Marked as deleted by ICDD
Subfiles:	Inorganic
	Mineral
Quality:	Blank (B)

Comments

Deleted by:	Berry parcel of March 31, 1958.
Color:	Brassy yellow

References

Primary reference: Hanawalt. et al., Anal. Chem., 10, 475, (1938)

Optical data: Dana's System of Mineralogy, 7th Ed.

Unit cell: Dana's System of Mineralogy, 7th Ed.

Stick Pattern

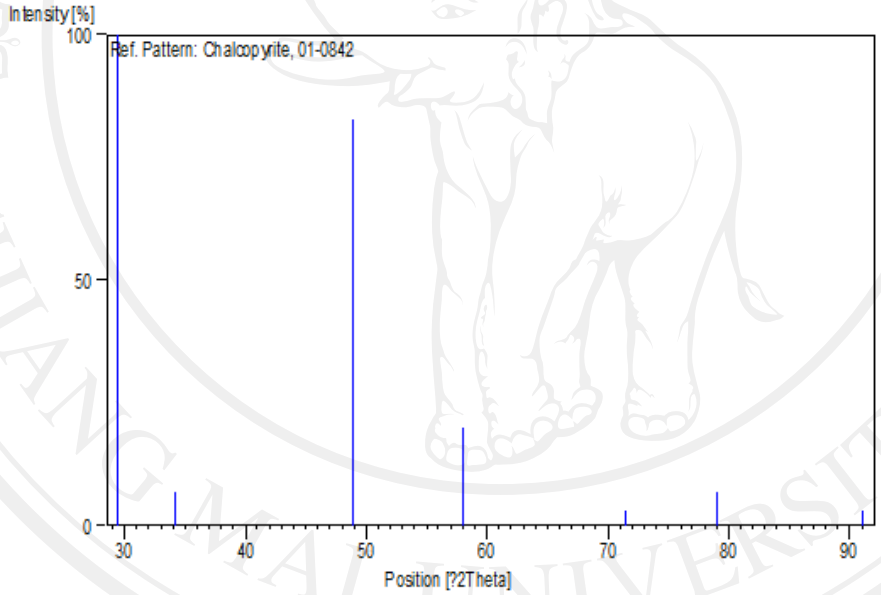

Peak list

No.	h	k	l	d [A]	I [%]
1	1	1	2	3.03000	100.0
2	2	0	0	2.62000	7.0
3	2	2	0	1.86000	83.0
4	3	1	2	1.59000	20.0

5	4	0	0	1.32000	3.0
6	3	3	2	1.21000	7.0
7	4	1	5	1.08000	3.0

APPENDIX B

Camera constant used for the indexing of SAED pattern

Table appendix B. Camera constant (Lλ) at 200 kV of JEOL - JEM-2010

L (cm)	D111Au (mm)	r111Au (mm)	D111Auv(A)	Lλ(mm.augstrom)
40	8.70	4.35	2.355	10.2442
60	13.2	6.60	2.355	15.5430
80	17.2	8.60	2.355	20.2530
100	21.2	10.60	2.355	24.963
120	25.2	12.60	2.355	29.6730
150	31.5	15.75	2.355	37.0912
200	41.5	20.75	2.355	48.8662
250	51.8	25.90	2.355	60.9945

CURRICULUM VITAE

Name Miss Kamonwan Aup-ngoen

Date of Birth 1st July 1985

Educational Background B.S. (Chemistry), Chiang Mai University, Chiang Mai, GPAx : 3.54 (honor)

Scholarship

2008-2013 the Thailand Research Fund (TRF) through The Royal Golden Jubilee Ph.D. Program (RGJ) (http://rgj.trf.or.th/eng/rgje21.asp) which supports the budget for Ph.D. program for 5 years

2004-2007 Research Professional Development Project under the Science Achievement Scholarship of Thailand (SAST) which supports the budget for Bachelor program for 4 years

Working/Training Experience

1. Training as a visiting researcher at Monash University, Melbourne, Australia from October 2011- July 2012 with the research topic as Application of Cu_3BiS_3 in Dye-sensitized Solar Cell
2. Workshop on Atomic Force Microscope (AFM), August 9-10, 2009 organized by Nanomaterials Research Unit, Faculty of Science, Chiang Mai University, Thailand
3. Training as a quality control officer at Aditya Birla Chemicals (Thailand) Ltd., Rayong, Thailand since March-May, 2007

International Conferences

1. Kamonwan Aup-Ngoen, Somchai Thongtem, Titipun Thongtem, "Cyclic microwave-assisted synthesis and characterization of flower-like Cu_3SbS_4", was presented at The 12th International Symposium on Eco-Materials Processing and Design (ISEPD 2011), January 8-11, 2011, Chiang Mai, Thailand
2. Somchai Thongtem, Kamonwan Aup-Ngoen, Titipun Thongtem, "Biomolecule and cyclic microwave radiation-assisted synthesis of Cu_3BiS_3 nanostructures crystals" was presented at The 11th International Symposium on Eco-Materials Processing and Design (ISEPD 2010), January 9-12, 2010, Osaka Prefecture University, Japan

Publications:

1. Kamonwan Aup-Ngoen, Somchai Thongtem, Titipun Thongtem , "Cyclic microwave-assisted synthesis of Cu_3BiS_3 dendrites using l-cysteine as a sulfur source and complexing agent", *Materials Letters*, Volume 65, Issue 3, 15 February 2011, Pages 442-445
2. Kamonwan Aup-Ngoen, Titipun Thongtem, Somchai Thongtem, "Characterization of Cu_3SbS_4 microflowers produced by a cyclic microwave radiation", *Materials Letters*, Volume 66, Issue 1, 1 January 2012, Pages 182-186
3. Kamonwan Aup-Ngoen, Titipun Thongtem, Somchai Thongtem, "Cyclic microwave-assisted synthesis of $CuFeS_2$ nanoparticles using biomolecules as sources of sulfur and complexing agent", *Materials Letters*, Volume 101, 15 June 2013, Pages 9-12

Materials Letters 65 (2011) 442–445

Contents lists available at ScienceDirect

Materials Letters

journal homepage: www.elsevier.com/locate/matlet

Cyclic microwave-assisted synthesis of Cu_3BiS_3 dendrites using L-cysteine as a sulfur source and complexing agent

Kamonwan Aup-Ngoen [a], Somchai Thongtem [a,*], Titipun Thongtem [b]

[a] Department of Physics and Materials Science, Faculty of Science, Chiang Mai University, Chiang Mai 50200, Thailand
[b] Department of Chemistry, Faculty of Science, Chiang Mai University, Chiang Mai 50200, Thailand

ARTICLE INFO

Article history:
Received 27 August 2010
Accepted 7 October 2010
Available online 29 October 2010

Keywords:
Characterization methods
Luminescence
Nanomaterials
Solar energy materials
X-ray techniques

ABSTRACT

Nanostructured Cu_3BiS_3 dendrites were successfully synthesized from CuCl, $BiCl_3$ and L-cysteine in ethylene glycol (EG), using cyclic microwave radiation (CMR). The phase was detected by X-ray diffraction (XRD) and selected area electron diffraction (SAED), and was in accordance with that obtained by the simulation. Scanning and transmission electron microscopic (SEM and TEM) techniques revealed the gradual transformation of nanoparticles to nanostructured dendrites, due to the increase of microwave power. Photoluminescence of Cu_3BiS_3 dendrites was a blue emission centered at 367 nm.

1. Introduction

Due to the linear and non-linear properties of I-V-VI ternary compounds, a number of studies have been devoted to the technological applications of these semiconducting materials. They have a high potential for use as optoelectronic and thermoelectric devices, including optical recording media [1]. Copper bismuth sulfide (Cu_3BiS_3), with the mineral name wittichenite [2], is one of the promising materials for use as p-type semiconductors [3,4], and as solar absorbers in photovoltaic devices [5]. It can be synthesized by different methods: powders in the polyacrylic acid matrix [3]; nanorods via a simple ethanol-thermal route [4]; thin films by reactive sputter deposition on hot substrates [5]; nanocrystallines by a hydrothermal decomposition process [6]; and others.

Microwaving is a process used for the synthesis of nanostructured materials. It can solve the problems of temperature and concentration gradients, and provides uniform growth media. By focusing microwave radiation into solutions, the vibrating electric field applies a force on dissolving species to induce vibrations with different modes. The processing is more rapid and efficient than that achieved by a conventional one, even at a low microwave power [7,8]. To avoid over-boiling, CMR was used instead of continuous.

Our motivation was to synthesize novel Cu_3BiS_3 dendritic crystals using a genetically coded amino acid (L-cysteine) by CMR. No one has ever succeeded in synthesizing Cu_3BiS_3 dendrites by this process.

2. Experiment

To synthesize nanostructured Cu_3BiS_3 dendrites, 3 mmol CuCl and 1 mmol $BiCl_3$ were dissolved in 30 ml EG to form a solution. Then 3 mmol L-cysteine ($C_3H_7NO_2S$) was added with 30 min continuous stirring. Samples of the solution were irradiated using 300–700 W CMR (30 s on for every 30 s interval) for 40 cycles. Finally, precipitates were synthesized, separated by filtration, washed with de-ionized water and absolute ethanol, and dried at 70 °C for 24 h, for further characterization.

3. Results and discussion

Fig. 1 shows XRD patterns of the products synthesized by 300–700 W CMR. At 300 W, the XRD pattern was composed of rather broad peaks, specifying that the product's degree of crystallinity was quite low. Comparing the XRD pattern to the JCPDS database (nos. 43-1479 and 02-1272) [2], this product was proved to be orthorhombic Cu_3BiS_3 mixed with Cu_2S impurity. The strongest intensity peak at 31.3° was found to correspond with the (131) crystallographic plane of the Cu_3BiS_3 phase, which was specified as the main product. When the microwave power was increased, the XRD pattern became sharper. At 700 W, the pattern was composed of the sharpest peaks. At this stage, the degree of crystallinity was the highest — implying that the atoms had arranged themselves in the best order. By increasing microwave power, the impurities were lessened as well. Until microwaving at powers of 600 and 700 W, the products were pure single-phase orthorhombic Cu_3BiS_3.

SEM and TEM images show nanostructured Cu_3BiS_3 synthesized using different microwave powers. At 300 W, the product (Fig. 2a)

* Corresponding author. Tel.: +66 53941922; fax: +66 53943445.
E-mail address: schthongtem@yahoo.com (S. Thongtem).

0167-577X/$ – see front matter © 2010 Elsevier B.V. All rights reserved.
doi:10.1016/j.matlet.2010.10.047

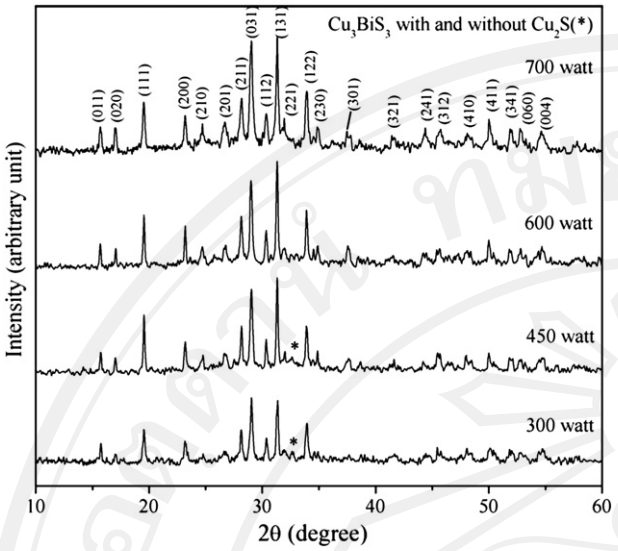

Fig. 1. XRD patterns of Cu_3BiS_3 synthesized at different microwave powers.

was composed of a number of nanoparticles with different orientations. By increasing the powers from 300 W to 450 and 600 W (Fig. 2b, c,and Fig. 3a,c), some of the products were gradually transformed into dendrites. At these stages, the products were mixtures of nanoparticles and dendrites. It should be noted that their morphologies shown on SEM images are in three dimensions, but those on TEM images are in two dimensions. At 700 W (Figs. 2d and 3e), the whole product consisted of dendrites with different orientations. This phenomenon proved that microwave radiation at higher powers has a strong influence on vibrating atoms to form a crystal lattice, and that orthorhombic Cu_3BiS_3 unit cells were able to arrange themselves to fit with both nanoparticles and dendrites. When a dendrite, produced at 700 W, was characterized using HRTEM (Fig. 3f,g), a number of the (011) planes 5.6 Å apart were detected — implying that the dendrite was single crystal. SAED patterns of the whole products, synthesized using 450, 600, and 700 W (Fig. 3b,d,and h), appear as concentric rings of bright spots of polycrystals; but that of a dendrite synthesized at 700 W (Fig. 3i) was composed of systematic spots of diffraction electrons from a single crystal. The patterns for both polycrystals and single crystal were interpreted [9], and specified as orthorhombic Cu_3BiS_3 [2], with the electron beam for the interpretation of Fig. 3i in the [4-3-5] direction. No Cu_2S impurity was detected in the SAED pattern of the product synthesized at 450 W, due to the very low Cu_2S concentration in this host. An electron diffraction pattern (Fig. 3j) was also simulated [10], using the [4-3-5] direction as a zone axis. It appears as a systematic array of spots, corresponding to that obtained by the interpretation of Fig. 3i — showing that this electron diffraction pattern of the product could exist in reality.

In this research, CuCl and $BiCl_3$ were dissolved in EG to form a solution. L-cysteine, a genetically coded amino acid, was used as a sulfur source and complexing agent. By adding L-cysteine to the solution, Cu^+ and Bi^{3+} ions coordinated with it to form complexes.

$$Cu^+ + \text{L-cysteine} \xrightarrow{\text{coordination}} [\text{Cu(L-cysteine)complexes}]$$

$$Bi^{3+} + \text{L-cysteine} \xrightarrow{\text{coordination}} [\text{Bi(L-cysteine)complexes}]$$

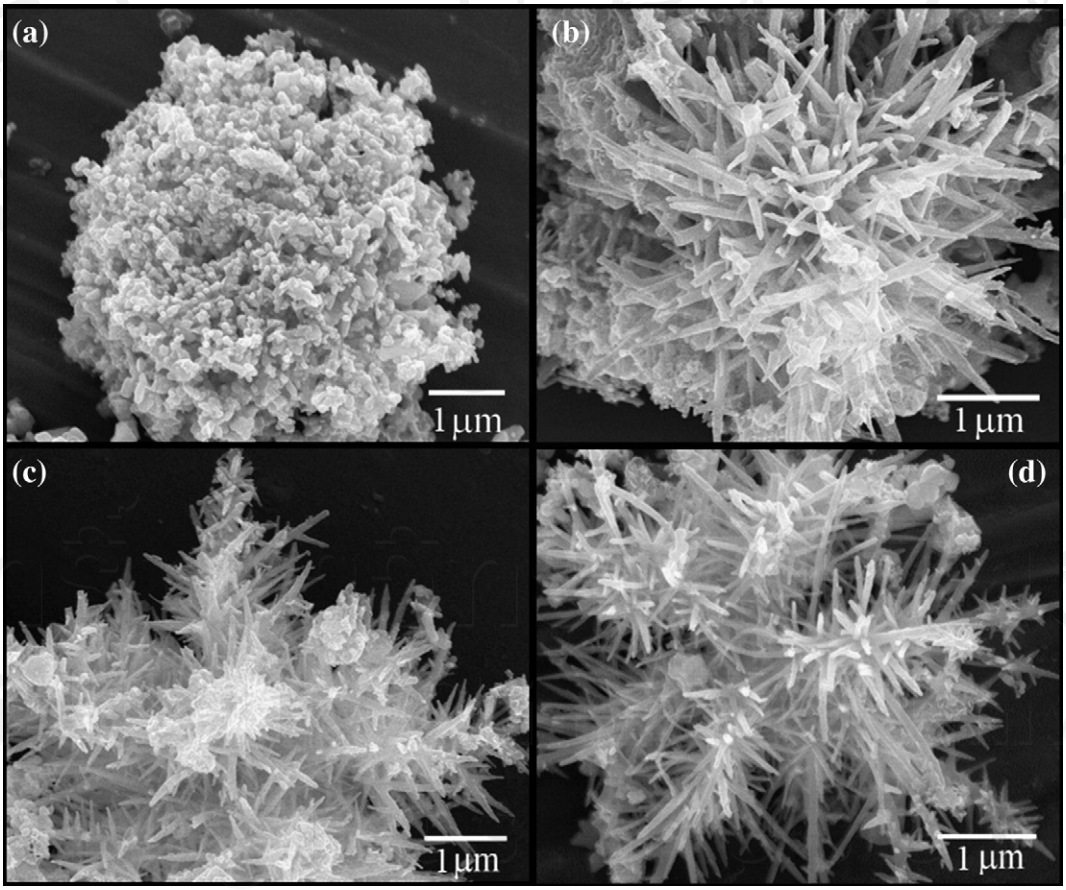

Fig. 2. SEM images of Cu_3BiS_3 synthesized at (a–d) 300, 450, 600, and 700 W, respectively.

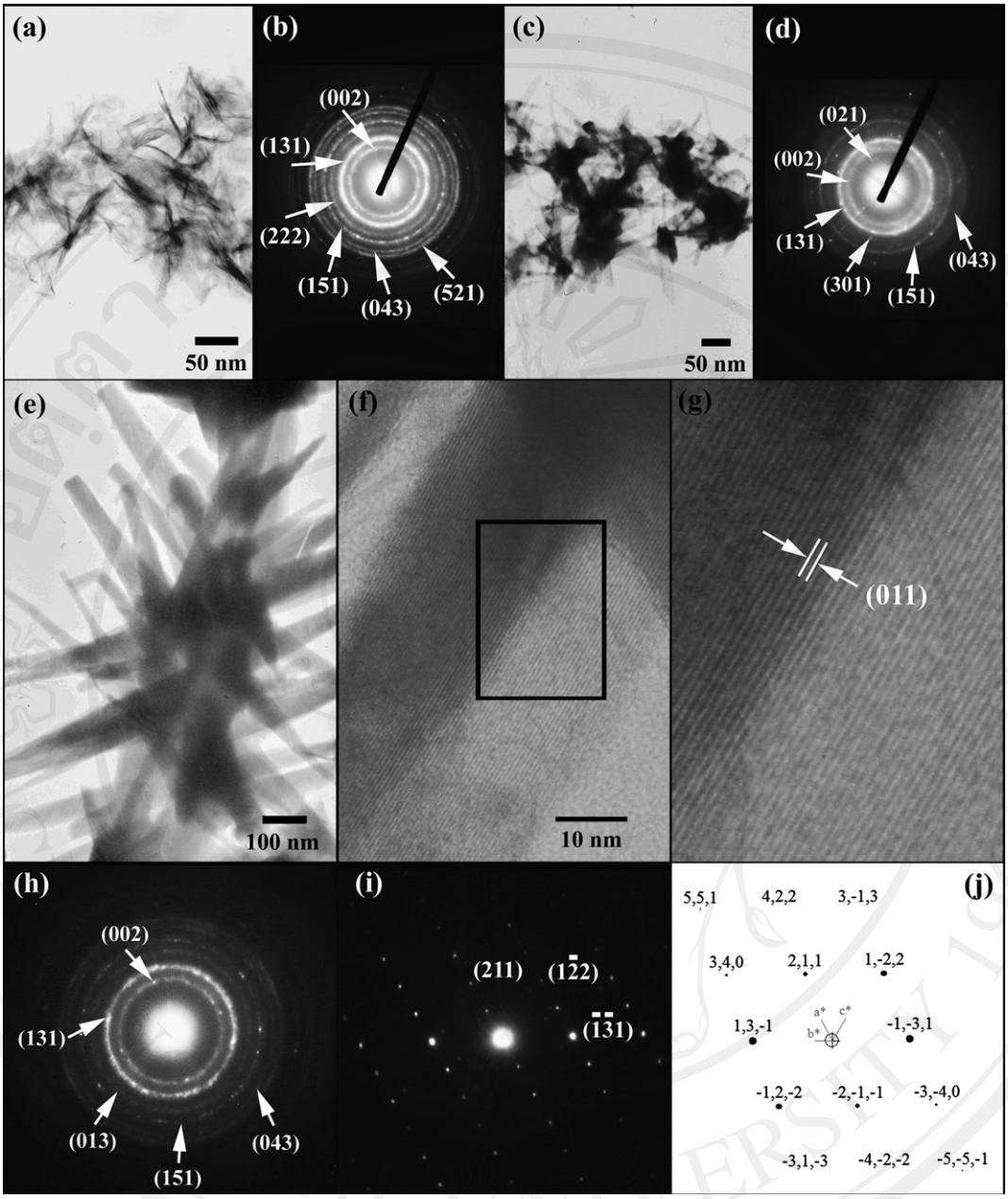

Fig. 3. TEM and HRTEM images, and SAED patterns of Cu_3BiS_3 synthesized at (a, b) 450 W, (c, d) 600 W, and (e–i) 700 W. (j) Simulated pattern of (i).

Under 700 W CMR, these complexes decomposed, and Cu_3BiS_3 nuclei were synthesized very rapidly. At this stage, the number of free ions was very low. Thus, Cu_2S and Bi_2S_3 formations were inhibited [1,11,12].

$$[\text{Cu(L-cysteine)complexes}] + [\text{Bi(L-cysteine)complexes}] \xrightarrow{\textit{decomposition}} Cu_3BiS_3(\text{nuclei})$$

Concurrently, [Cu–Bi(L-cysteine) complexes] could possibly form by the reaction

$$Cu^{+} + Bi^{3+} + \text{L-cysteine} \xrightarrow{\textit{coordination}} [\text{Cu-Bi(L-cysteine)complexes}].$$

These complexes were then decomposed by CMR.

$$[\text{Cu-Bi(L-cysteine)complexes}] \xrightarrow{\textit{decomposition}} Cu_3BiS_3(\text{nuclei}).$$

These nuclei grew to synthesize Cu_3BiS_3 dendrites. Dendritic growth was promoted by the strong atomic vibrations. Thus these atoms had more chances to arrange themselves in perfect order to form dendritic crystals. In the present research, CMR played a key role in the growth of Cu_3BiS_3 crystals: both in the decomposition of the complexes, and in the nucleation and growth of Cu_3BiS_3. By using CMR, the process is rapid and homogenous, providing a uniform growth environment; thus crystalline dendrites were rapidly synthesized. At 300 W CMR, the nucleation rate of Cu_3BiS_3 was slower; Cu_2S at a very low concentration thus had a better chance to nucleate as a second phase contained in this nanoparticle product.

Photoluminescence (PL) of Cu_3BiS_3 dendrites was studied at room temperature, using 300 nm excitation wavelength from a xenon laser. The spectrum (Fig. 4) was blue emission centered at 367 nm, with the shoulder at 412 nm (caused by some defects that originated during the synthesis process). These Cu_3BiS_3 dendrites were I-V-VI ternary promising materials for use in solar energy converters and optical nanodevices.

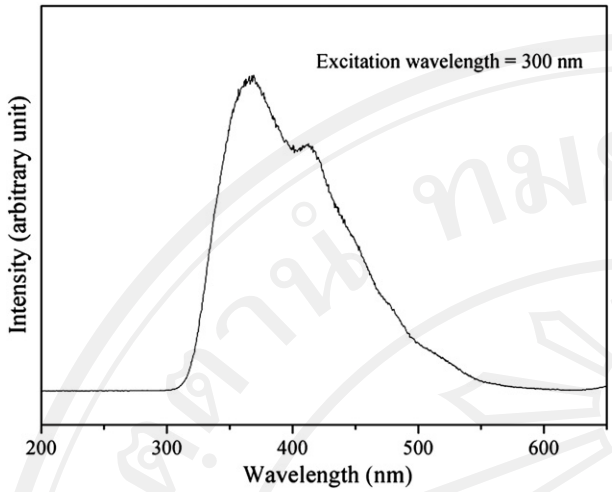

Fig. 4. PL emission of Cu_3BiS_3 dendrites synthesized at 700 W.

4. Conclusions

Nanostructured Cu_3BiS_3 dendrites were successfully synthesized by CMR. The phase was detected using XRD and SAED. SEM and TEM images showed that, with increasing microwave power, nanoparticles were gradually transformed into dendritic single crystals composed of a number of (011) parallel crystallographic planes. PL emission of the Cu_3BiS_3 dendrites was blue emission centered at 367 nm.

Acknowledgements

This research was supported by the Thailand Research Fund (TRF), and the National Nanotechnology Center (NANOTEC), a member of National Science and Technology Development Agency (NSTDA), Ministry of Science and Technology, Thailand.

References

[1] Jiasong Z, Weidong X, Huaidong J, Wen C, Lijun L, Xinyu Y, et al. L Mater Lett 2010;64:1499–502.
[2] Powder Diffract File, JCPDS-ICDD, 12 Campus Boulevard, Newtown Square, PA 19073-3273, U.S.A. 2001.
[3] Hu H, Gomez-Daza O, Nair PK. J Mater Res 1998;13:2453–6.
[4] Chen D, Shen G, Tang K, Liu X, Qian Y, Zhou G. J Cryst Growth 2003;253:512–6.
[5] Gerein NJ, Haber JA. Chem Mater 2006;18:6297–302.
[6] Hu J, Deng B, Wang C, Tang K, Qian Y. Mater Chem Phys 2003;78:650–4.
[7] Wang G, Hao C. Mater Res Bull 2009;44:418–21.
[8] Sczancoski JC, Cavalcante LS, Joya MR, Espinosa JWM, Pizani PS, Varela JA. J Colloid Interf Sci 2009;330:227–36.
[9] Andrews KW, Dyson DJ, Keown SR. Interpret Electr Diffract Pattern. 2nd ed. Plenum Press: New York; 1971.
[10] Boudias C, Monceau D. CaRIne Crystallography 3.1, DIVERGENT S.A. 60200 Compiègne, France: Centre de Transfert; 1989–1998.
[11] Thongtem T, Jaroenchaichana J, Thongtem S. Mater Lett 2009;63:2163–6.
[12] Chen D, Shen G, Tang K, Jiang X, Huang L, Jin Y, et al. Inorg Chem Commun 2003;6:710–2.

Materials Letters 66 (2012) 182–186

Contents lists available at SciVerse ScienceDirect

Materials Letters

journal homepage: www.elsevier.com/locate/matlet

Characterization of Cu_3SbS_4 microflowers produced by a cyclic microwave radiation

Kamonwan Aup-Ngoen [a], Titipun Thongtem [b,c,*], Somchai Thongtem [a,c]

[a] Department of Physics and Materials Science, Faculty of Science, Chiang Mai University, Chiang Mai 50200, Thailand
[b] Department of Chemistry, Faculty of Science, Chiang Mai University, Chiang Mai 50200, Thailand
[c] Materials Science Research Center, Faculty of Science, Chiang Mai University, Chiang Mai 50200, Thailand

ARTICLE INFO

Article history:
Received 16 July 2011
Accepted 11 August 2011
Available online xxxx

Keywords:
Electron microscopy
Semiconductors
X-ray techniques

ABSTRACT

Copper antimony sulfide (Cu_3SbS_4) crystals were produced from mixtures of different molar ratios of CuCl, $SbCl_3$ and thiourea in 40 and 60 ml ethylene glycol (EG) by a 300 W cyclic microwave radiation (CMR) for different lengths of time. In the present research, tetragonal Cu_3SbS_4 microflowers, characterized by X-ray and electron diffraction including electron microscopy and Raman analyses, were successfully produced in the 40 ml solution containing 2:2:4 molar ratio Cu:Sb:S for 40 cycles. Their UV-visible absorption was studied to determine the energy gap (E_g). A formation mechanism was also proposed to relate with the experimental results.

1. Introduction

Recently, scientists and engineers pay much attention to semiconducting chalcogenide materials, due to their different applications in optoelectronic, photovoltaic, and thermoelectric technologies [1–3]. Cu_3SbS_4 is a I-V-VI ternary compound with non-linear optical properties [1,2]. Traditionally, ternary chalcogenides were produced by solid state reactions [4]. Until now, there are a few reports on the synthesis of Cu_3SbS_4: microscale particles via an adjusted polyol-route [1], and high quality nanofibers through a mild hydrothermal route [2]. Our motivation is to produce Cu_3SbS_4 microflowers by a CMR, without adding any additives - a rapid process with low temperature and non-toxic chemical requirements.

2. Experiment

By separate dissolving of CuCl and $SbCl_3$ in EG, and followed by thiourea (NH_2CSNH_2, TU) adding, these solutions were thoroughly mixed to form 40 and 60 ml mixtures. In this research, a 300 W CMR (40 s on for every 40 s interval) proceeded for 40, 30, 20, 10, and 2 cycles, and different molar ratios of Cu:Sb:S were 3:1:4 (A), 3:1:5 (B), 3:1:6 (C), 3:2:4 (D), 3:3:4 (E), 2:2:4 (F), and 1:1:4 (G). Finally, the precipitates were washed with absolute ethanol, and dried at 70 °C for 24 h for further analyses.

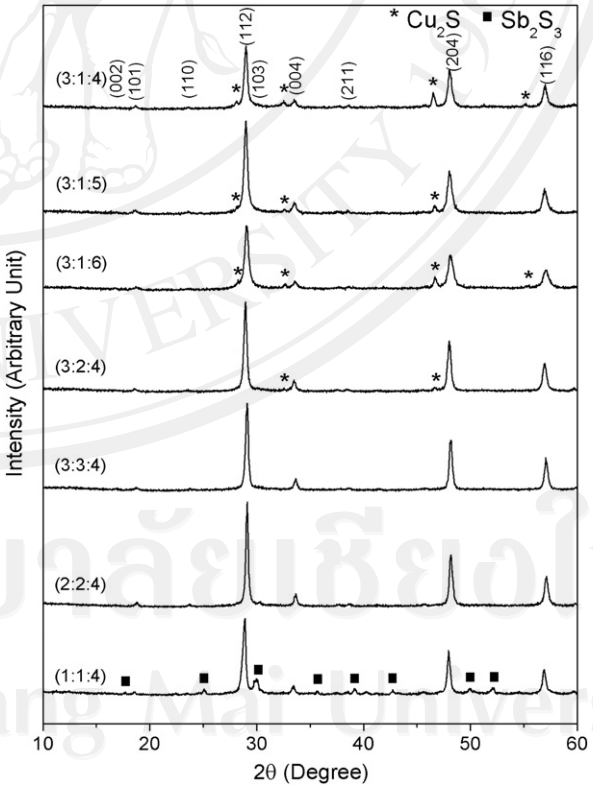

Fig. 1. XRD patterns of Cu_3SbS_4 produced from different molar ratios of Cu:Sb:S in 40 ml EG by 300 W CMR for 40 cycles.

* Corresponding author at: Department of Chemistry, Faculty of Science, Chiang Mai University, Chiang Mai 50200, Thailand. Tel.: +66 53943344; fax: +66 53892277.
E-mail addresses: ttpthongtem@yahoo.com, ttpthongtem@gmail.com (T. Thongtem).

0167-577X/$ – see front matter © 2011 Elsevier B.V. All rights reserved.
doi:10.1016/j.matlet.2011.08.035

3. Results and discussion

3.1. XRD

XRD patterns (Fig. 1) of the products, produced using different molar ratios of Cu:Sb:S, were compared with the JCPDS database nos 10–0472 (Cu_3SbS_4), 02–1284 (Cu_2S), and 71–2432 (Sb_2S_3) [5]. Both Cu_3SbS_4 and Cu_2S impurity were detected in the A, B, C, and D powders, due to the excessive Cu^{+} and S^{2-}. For 3:3:4 (E) and 2:2:4 (F) molar ratios of Cu:Sb:S, pure tetragonal Cu_3SbS_4 was detected. Some sulfur was likely to be left in the products, and washed out by ethanol. But for the 1:1:4 molar ratio Cu:Sb:S (G), Cu_3SbS_4 and Sb_2S_3 impurity were detected – caused by the excessive Sb^{3+} and S^{2-}.

3.2. SEM, TEM, EDX and SAED

Figs. 2–4 show typical image, elemental and phase analyses of Cu_3SbS_4 produced from 2:2:4 and 3:3:4 molar ratios of Cu:Sb:S in 40 and 60 ml EG by a 300 W CMR for 2–40 cycles. At 2:2:4 molar ratio Cu:Sb:S in 40 ml EG for 40 cycles CMR, the product was Cu_3SbS_4 black microflowers (Figs. 2a-c and 4a) with their petals formed by clustering of different particles. EDX analysis (Fig. 2d) revealed the presence of Cu, Sb, and S as the fundamental elements of these flowers, including sputtered Au to improve the conductivity for SEM analysis. Upon increasing the molar ratio from 2:2:4 to 3:3:4, the product became clusters of irregular particles with different orientations (Figs. 2e and 4f) – caused by the limited space for their growth. By adding EG until its content was 60 ml (Fig. 2f), different flower-like particles were reproduced. Upon lowering the processing time of the F mixture from 40 cycles to 30, 20, and 10 cycles, the products (Fig. 3a-f) produced from 2:2:4 molar ratio Cu:Sb:S remained as black microflowers, with reducing sizes in sequence. Until for 2 cycles, the product (Fig. 3g and h) was white rectangular sticks.

For the product produced from 2:2:4 molar ratio Cu:Sb:S in 40 ml EG, the SAED pattern (Fig. 4d) was interpreted [6] and specified as tetragonal Cu_3SbS_4[5]. It was in good accordance with that obtained by simulation (Fig. 4e) [7], although some spots of the interpreted pattern did not appear on the simulated one – due to the following. To simulate the pattern, intensity and size of the spots (planes) were mutually related. The stronger intensity was used, the larger size was achieved. The intensity and size of the spots were limited by a saturated intensity used for simulation. Thus some planes of the JCPDS database with low intensity did not appear in the simulated pattern. The (110) and (103) lattice planes (Fig. 4b and c) were detected as parallel stripes, composing Cu_3SbS_4 crystals. A SAED pattern (Fig. 4g) of the product produced from 3:3:4 molar ratio Cu:Sb:S

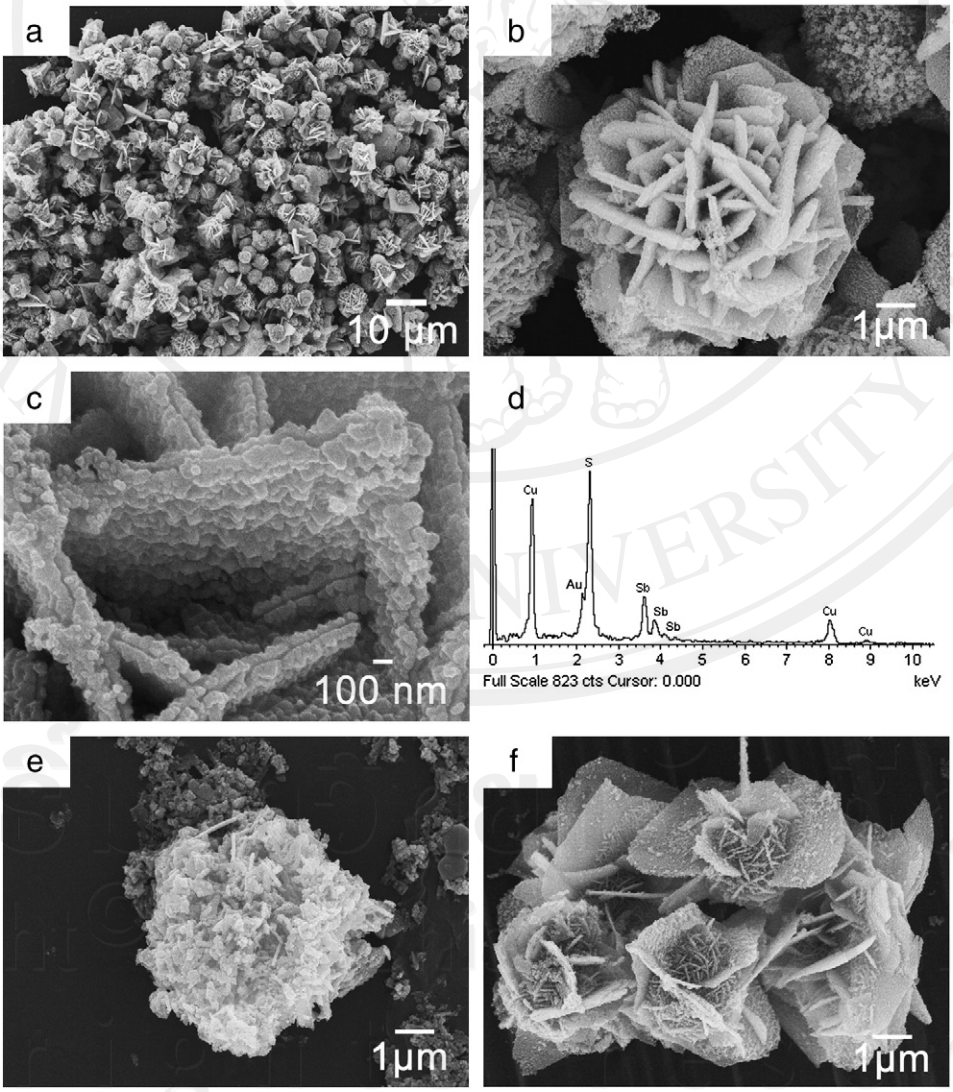

Fig. 2. SEM and EDX analyses of Cu_3SbS_4 produced by 300 W CMR for 40 cycles. (a-d) 2:2:4 molar ratio Cu:Sb:S in 40 ml EG, and (e, f) 3:3:4 molar ratio Cu:Sb:S in 40 and 60 ml EG, respectively.

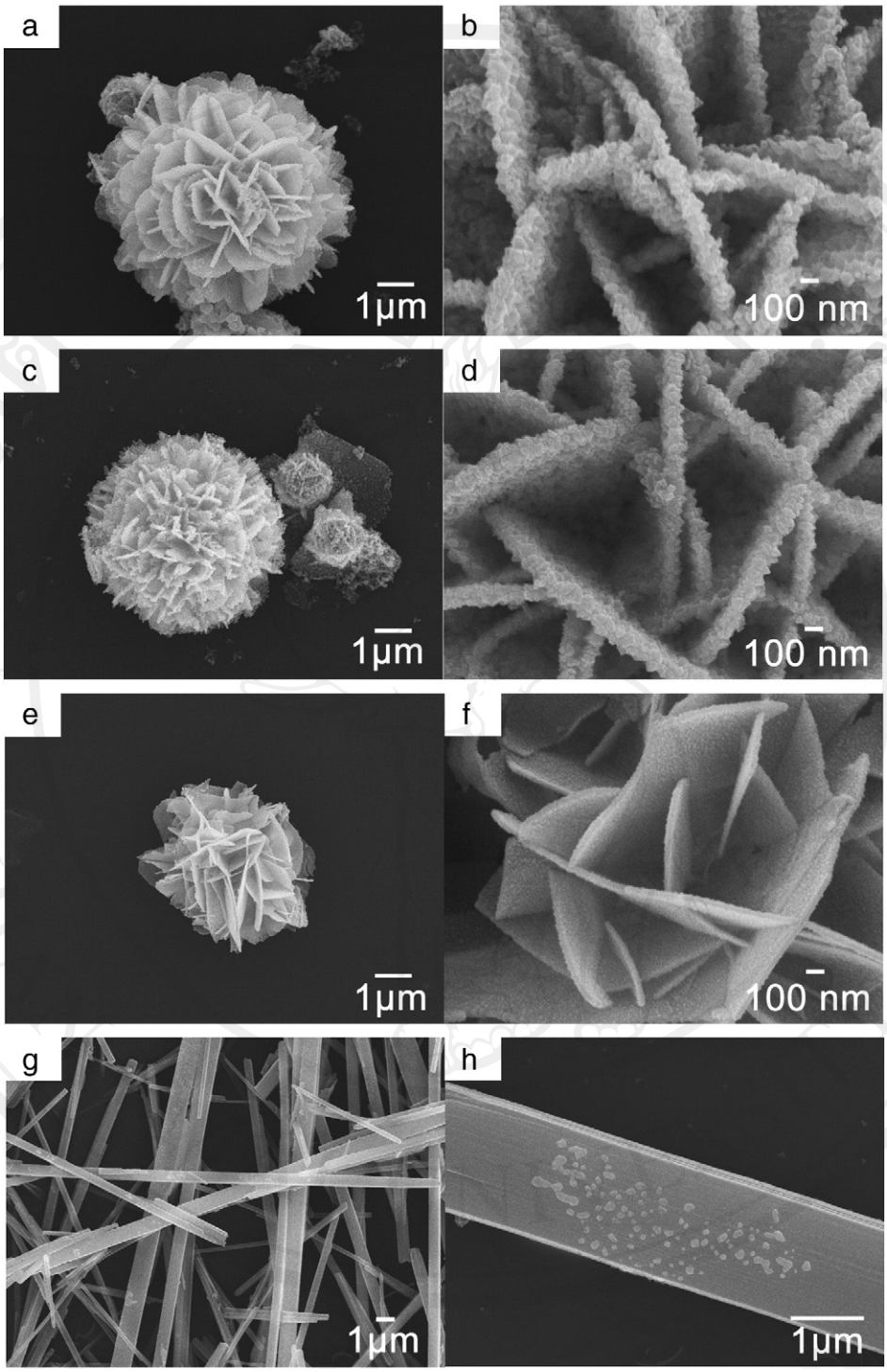

Fig. 3. SEM images of Cu_3SbS_4 produced from 2:2:4 molar ratio Cu:Sb:S in 40 ml EG by 300 W CMR for (a, b) 30, (c, d) 20, (e, f) 10, and (g, h) 2 cycles.

in 40 ml EG was composed of bright spots of diffuse concentric rings, specified as polynanocrystalline Cu_3SbS_4 [5].

4. Formation mechanism

To produce Cu_3SbS_4, $CuCl + TU$ and $SbCl_3 + TU$ solutions were mixed. Thus complexes were possibly formed.

$$Cu^{+} + TU \rightarrow Cu - TU \text{ complexes}$$

$$Sb^{3+} + TU \rightarrow Sb - TU \text{ complexes}$$

They were mixed, and processed by a CMR to produce Cu_3SbS_4 [8,9].

$$Cu - TU \text{ complexes} + Sb - TU \text{ complexes} \rightarrow Cu_3SbS_4 \text{ (nuclei)}$$

Alternatively, Cu-Sb-TU complexes could also form.

$$Cu^{+} + Sb^{3+} + TU \rightarrow Cu - Sb - TU \text{ complexes}$$

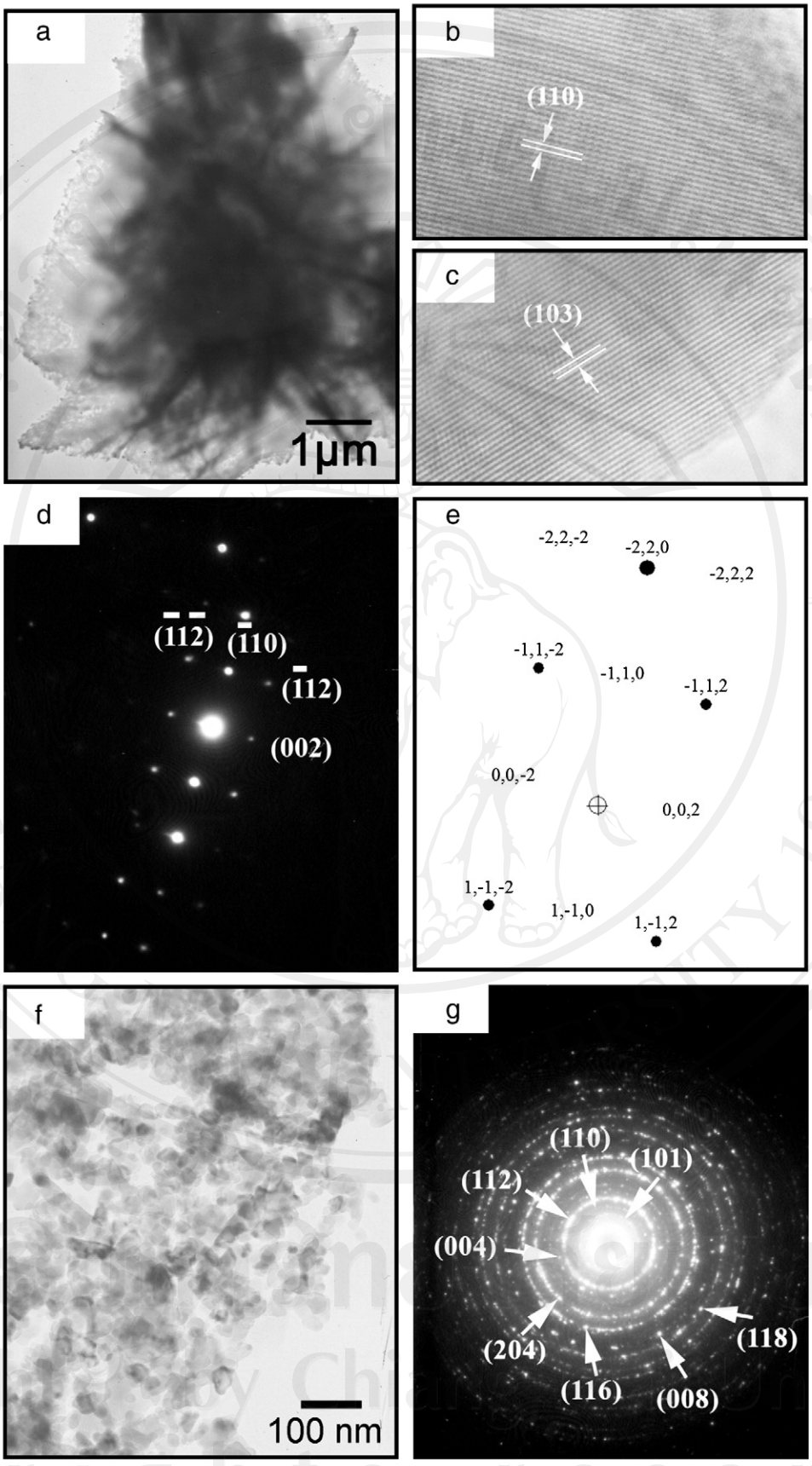

Fig. 4. TEM and HRTEM images, and SAED and simulated patterns of Cu_3SbS_4 produced by 300 W CMR for 40 cycles. (a-e) 2:2:4, and (f, g) 3:3:4 molar ratios of Cu:Sb:S in 40 ml EG.

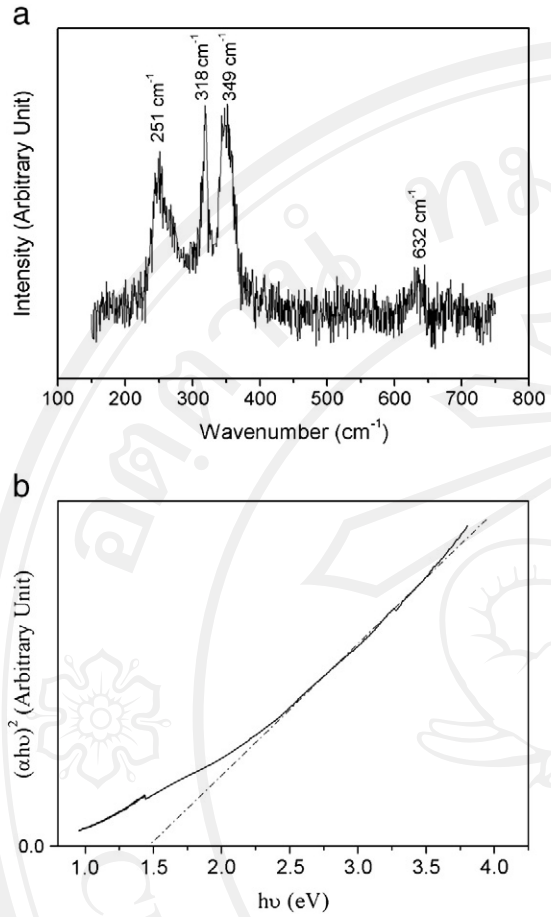

Fig. 5. (a) Raman shifts and (b) UV-visible absorption of Cu_3SbS_4 produced from 2:2:4 molar ratio Cu:Sb:S in 40 ml EG by 300 W CMR for 40 cycles.

Cu_3SbS_4 nuclei were produced by CMR.

$$Cu - Sb - TU \text{ complexes} \rightarrow Cu_3SbS_4 \text{ (nuclei)}$$

During processing for 10–40 cycles, the nuclei grew to form pure nanostructured flowers (F mixture).

When the contents of Cu^+ and S^{2-} were excessive, Cu_2S impurity was produced.

$$2Cu^+ + S^{2-} \rightarrow Cu_2S$$

Sb_2S_3 could also form, due to the excess of Sb^{3+} and S^{2-}.

$$2Sb^{3+} + 3S^{2-} \rightarrow Sb_2S_3$$

5. Raman and UV-visible spectroscopy

By using 50 mW Ar green laser (514.5 nm wavelength), four Raman shifts of Cu_3SbS_4 (Fig. 5a) produced from 2:2:4 molar ratio Cu:Sb:S in 40 ml EG by 300 W CMR for 40 cycles were at 251, 318, 349, and 632 cm^{-1} – in accordance with the previous report [10]. The 318 and 632 cm^{-1} peaks seemed to correspond with the fundamental and overtone modes, respectively. Its UV-visible absorption (Fig. 5b) was controlled by two photon energy ($h\nu$) range. For $h\nu > E_g$, the curve for direct interband transitions was linearly increased with the increasing of $h\nu$. Its inclination was caused by the absorption for charged transition from the topmost occupied state of valence band to the bottommost unoccupied state of conduction band. For $h\nu < E_g$, the curve was different from linearity, caused by absorption relating to defects [11]. The direct E_g, determined by extrapolating the linear portion curve to zero absorption, was 1.47 eV - a promising E_g for multiple potential applications. It was in the same range as E_g (300 K, absorption) = 1.24 eV of Cu_3AsS_4[12], and E_g = 1.4 eV of $CuSbS_2$ thin film heated at 150 °C [13].

6. Conclusions

Pure tetragonal Cu_3SbS_4 microflowers were produced from 2:2:4 molar ratio Cu:Sb:S in 40 ml EG, by a 300 W CMR for 40 cycles. Crystalline phase, composition, morphology and atomic vibrations were specified by XRD, EDX, SEM, TEM, SAED, and Raman analyses. A possible formation mechanism of Cu_3SbS_4 was also proposed in accordance with the experimental results.

Acknowledgements

We wish to thank the National Nanotechnology Center (NANOTEC), National Science and Technology Development Agency, Thailand, for financial support through the project code: P-10-11345, Thailand's Office of the Higher Education Commission through the National Research University Project, and Thailand Research Fund through the RGJ Ph.D. Program, including Graduate School of Chiang Mai University for general support.

References

[1] Blöß S, Jansen M. Z Naturforsch 2003;58b:1075–8.
[2] An Ch, Jin Y, Tang K, Qian Y. J Mater Chem 2003;13:301–3.
[3] Jiasong Z, Weidong X, Huaidong J, Wen C, Lijun L, Xinyu Y, et al. Mater Lett 2010;64:1499–502.
[4] Garin J, Parthé E. Acta Cryst 1972;B28:3672–4.
[5] Powder Diffract. File, JCPDS-ICDD, 12 Campus Boulevard, Newtown Square, PA 19073–3273, U.S.A. 2001.
[6] Andrews KW, Dyson DJ, Keown SR. Interpret Electr Diffract Pattern. 2nd ed. Plenum Press: New York; 1971.
[7] Boudias C, Monceau D. CaRIne Crystallography 3.1, DIVERGENT S.A. 60200 Compiègne, France: Centre de Transfert; 1989–1998.
[8] Aup-Ngoen K, Thongtem S, Thongtem T. Mater Lett 2011;65:442–5.
[9] Chen D, Shen G, Tang K, Jiang X, Huang L, Jin Y, et al. Inorg Chem Commun 2003;6:710–2.
[10] http://rruff.info/Famatinite/R110022.
[11] Sungpanich J, Thongtem T, Thongtem S. Mater Lett 2011;65:3000–4.
[12] http://www.springermaterials.com/docs/info/10717201_165.html.
[13] Rabhi A, Kanzari M, Rezig B. Thin Solid Films 2009;517:2477–80.

Materials Letters 101 (2013) 9–12

Contents lists available at SciVerse ScienceDirect

Materials Letters

journal homepage: www.elsevier.com/locate/matlet

Cyclic microwave-assisted synthesis of $CuFeS_2$ nanoparticles using biomolecules as sources of sulfur and complexing agent

Kamonwan Aup-Ngoen [a], Titipun Thongtem [b,c,*], Somchai Thongtem [a,c,**], Anukorn Phuruangrat [d]

[a] Department of Physics and Materials Science, Faculty of Science, Chiang Mai University, Chiang Mai 50200, Thailand
[b] Department of Chemistry, Faculty of Science, Chiang Mai University, Chiang Mai 50200, Thailand
[c] Materials Science Research Center, Faculty of Science, Chiang Mai University, Chiang Mai 50200, Thailand
[d] Department of Materials Science and Technology, Faculty of Science, Prince of Songkla University, Hat Yai, Songkhla 90112, Thailand

ARTICLE INFO

Article history:
Received 24 November 2012
Accepted 11 March 2013
Available online 21 March 2013

Keywords:
Electron microscopy
Nanocrystalline materials
Spectroscopy
X-ray techniques

ABSTRACT

Copper iron sulfide ($CuFeS_2$) nanoparticles were successfully synthesized by a 300 W cyclic microwave radiation, exposing onto ethylene glycol containing $Cu(CH_3COO)_2$, $FeCl_3 \cdot 6H_2O$ or $FeCl_2 \cdot 4H_2O$ and L-cysteine biomolecules. X-ray diffraction (XRD), field emission scanning electron microscopy (FE-SEM), transmission electron microscopy (TEM), Raman spectrometry and X-ray photoelectron spectroscopy (XPS) revealed the presence of pure tetragonal chalcopyrite $CuFeS_2$ nanoparticles with valence states of Cu^+, Fe^{3+} and S^{2-} and four Raman shifts at 215.0–218.6, 280.2–281.4, 394.4–394.9 and 472.2–473.4 cm^{-1}. A formation mechanism of the products was also proposed according to the experimental results.

1. Introduction

Chalcopyrite copper iron sulfide ($CuFeS_2$) is a I–III–VI_2 ternary compound known as an antiferromagnetic semiconductor, which has narrow band gap (0.5–0.6 eV), very high Néel temperature (550 °C) and innovative electrical, optical and magnetic properties [1–5]. It has potential applications for cathodes of lithium-ion batteries [6], solar cells [1] and thermoelectric devices [5]. Different methods have been investigated for the synthesis of $CuFeS_2$: nanorods and nanoparticles by hydrothermal synthesis [1,7], single crystalline nanowires and hexagonal plate-like chalcopyrite by the solvothermal process [2,6], spherical and pyramidal nanocrystals by thermal decomposition and reaction of metal-dithiocarbamate or acetylacetonate precursors with sulfur in an organic solvent mixture [3], and a combination of mechanical alloying and spark plasma sintering [5].

In this research, cyclic microwave radiation was used for the synthesis of $CuFeS_2$ nanoparticles using L-cysteine biomolecules as sources of sulfur and complexing agent. The process is more rapid and efficient than that achieved by a conventional one. Additionally, it can solve the problems of temperature and concentration gradients and provide uniform growth media.

2. Experiment

To synthesize $CuFeS_2$, 1 mmol $Cu(CH_3COO)_2$, 3 mmol $FeCl_3 \cdot 6H_2O$ or $FeCl_2 \cdot 4H_2O$ and 2 mmol $C_3H_7NO_2S$ (L-cysteine) were mixed in 40 ml ethylene glycol (EG) to form solutions which were processed by a 300 W cyclic microwave radiation (CMR) for 5–40 cycles. Each cycle, microwave radiation was on for 40 s every 40 s interval. In the end, the precipitates were separated, rinsed and dried at 70 °C for 24 h to form CA-1 and CA-2 products, where CA, 1 and 2 were for those synthesized using $Cu(CH_3COO)_2$, $FeCl_3 \cdot 6H_2O$ and $FeCl_2 \cdot 4H_2O$, respectively.

3. Results and discussion

XRD: The crystalline structure and chemical composition of the as-synthesized products were characterized by XRD of which the patterns (Fig. 1) were compared with the JCPDS database no. 01-0842 [8]. All diffraction peaks of CA-1 and CA-2 were readily indexed to be tetragonal chalcopyrite $CuFeS_2$. Their XRD peaks were similar in height and very sharp, implying that the products were composed of a number of particles with the same size and high crystalline degree.

SEM, TEM, EDX and SAED: An effect of different iron sources on morphologies was investigated by SEM and EDX (Fig. 2). The CA-1

* Corresponding author at: Department of Chemistry, Faculty of Science, Chiang Mai University, Chiang Mai 50200, Thailand. Tel.: +66 53943344; fax: +66 53892277.
** Corresponding author at: Department of Physics and Materials Science, Faculty of Science, Chiang Mai University, Chiang Mai 50200, Thailand. Tel.: +66 53941924; fax: +66 53943445.
E-mail addresses: ttpthongtem@yahoo.com (T. Thongtem), schthongtem@yahoo.com, sthongtem@hotmail.com (S. Thongtem).

0167-577X/$ - see front matter © 2013 Elsevier B.V. All rights reserved.
http://dx.doi.org/10.1016/j.matlet.2013.03.055

product contained 10–20 nm nanoparticles in clusters. Each cluster appeared as rough surface which was the proof of loosely packed nanoparticles grouping together [9]. For the CA-2 product, it was composed of nanoparticles in irregular clusters, in accordance with the above XRD analysis. EDX spectra of both products revealed the presence of Cu, Fe and S as fundamental elements, sputtered Au for conductivity improving, including C and O of polymer tape.

The nanoparticles were further investigated by TEM and SAED (Fig. 3). For 40 cycles, intensive contrast at dark edges surrounding small bright areas indicates that CA-1 was composed of a number of nanoparticles cluster together, which was not able to be detected by SEM. The product presents really fine nanoparticles.

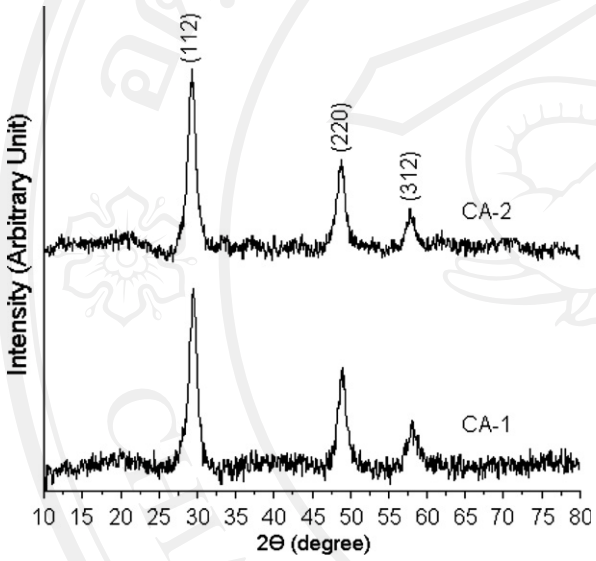

Fig. 1. XRD patterns of CA-1 and CA-2 synthesized for 40 cycles.

Upon decreasing the processing time from 40 cycles to 20 and 5 cycles, the products remained as clusters of nanoparticles with reducing their sizes in sequence. By changing the iron source from $FeCl_3 \cdot 6H_2O$ to $FeCl_2 \cdot 4H_2O$, clusters of nanoparticles were still detected. SAED patterns of these products were composed of diffuse and hollow concentric rings, specified as polynanocrystalline $CuFeS_2$ [8].

Raman and XPS spectra: Raman spectra of $CuFeS_2$ (Fig. 4) shows four Raman shifts at 215.0–218.6, 280.2–281.4 (A_1 modes), 394.4–394.9 (B_2 modes) and 472.2–473.4 (E modes) cm^{-1}, in accordance with the previous report [10]. A slight difference of Raman peaks was observed, caused by systematic downshift of Raman peaks of the CA-1 comparing with those of the CA-2. Band positions and relative intensities of the Raman peaks could slightly vary from one spectrum to another due to the orientation of crystal lattice and optical properties, including the presence of local impurities or defects inside [10,11].

XPS spectra of copper, iron and sulfur containing in CA-1 and CA-2 are shown in Fig. 5. The Cu2p core-level spectra show the analyzed binding energy (BE) of $Cu2p_{3/2}$ (932.3–932.5 eV) and $Cu2p_{1/2}$ (952.2–952.5 eV) peaks, corresponding to Cu^+. No $Cu2p_{3/2}$ satellite peak at 942 eV of Cu^{2+} was detected. For the Fe2p core-level spectra, BE of $Fe2p_{3/2}$ (711.3–711.5 eV) and $Fe2p_{1/2}$ (725.8–726.2 eV) were in good accordance with Fe^{3+}. The S2p core-level spectra reveal BE of $S2p_{3/2}$ (162.5–163.3 eV), corresponding to S^{2-} [2,3,12]. Furthermore, additional peaks were detected at 169.0–169.1 eV and were likely to be from the oxidized parts of the products during the synthesis. Other minor peaks of C1 s (284.5–285.3 eV) and O1 s (531.3–531.5 eV) were also detected [2]. They belonged to the coated carbon for conductivity improvement for XPS analysis and absorbed gaseous molecules.

Formation mechanism: Mixtures of $Cu(CH_3COO)_2$, $FeCl_3 \cdot 6H_2O$ and L-cysteine biomolecules in EG were processed by CMR to form $CuFeS_2$ with valence states of Cu^+, Fe^{3+} and S^{2-}. Possibly, $Cu(CH_3COO)_2$ was reduced by EG, a well-known reducing agent, by transforming Cu^{2+} into Cu^+ intermediate ions [13–16], which further combined with L-cysteine to form [Cu(L-cysteine) complexes]. Concurrently, Fe^{3+} formed [Fe(L-cysteine) complexes]

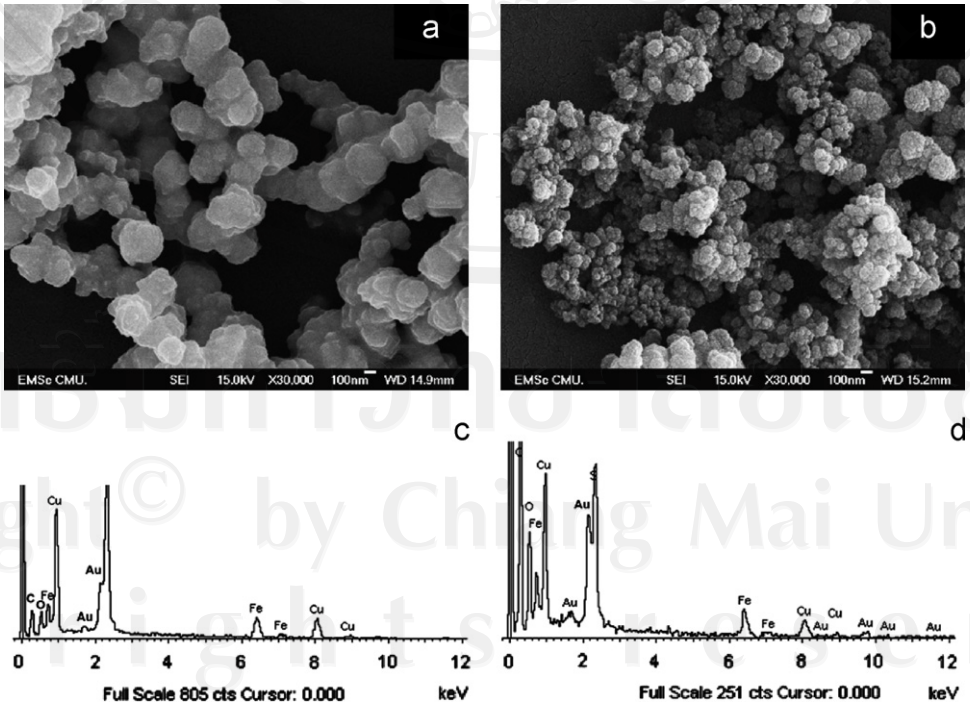

Fig. 2. SEM images and EDX spectra of (a,c) CA-1 and (b,d) CA-2 synthesized for 40 cycles.

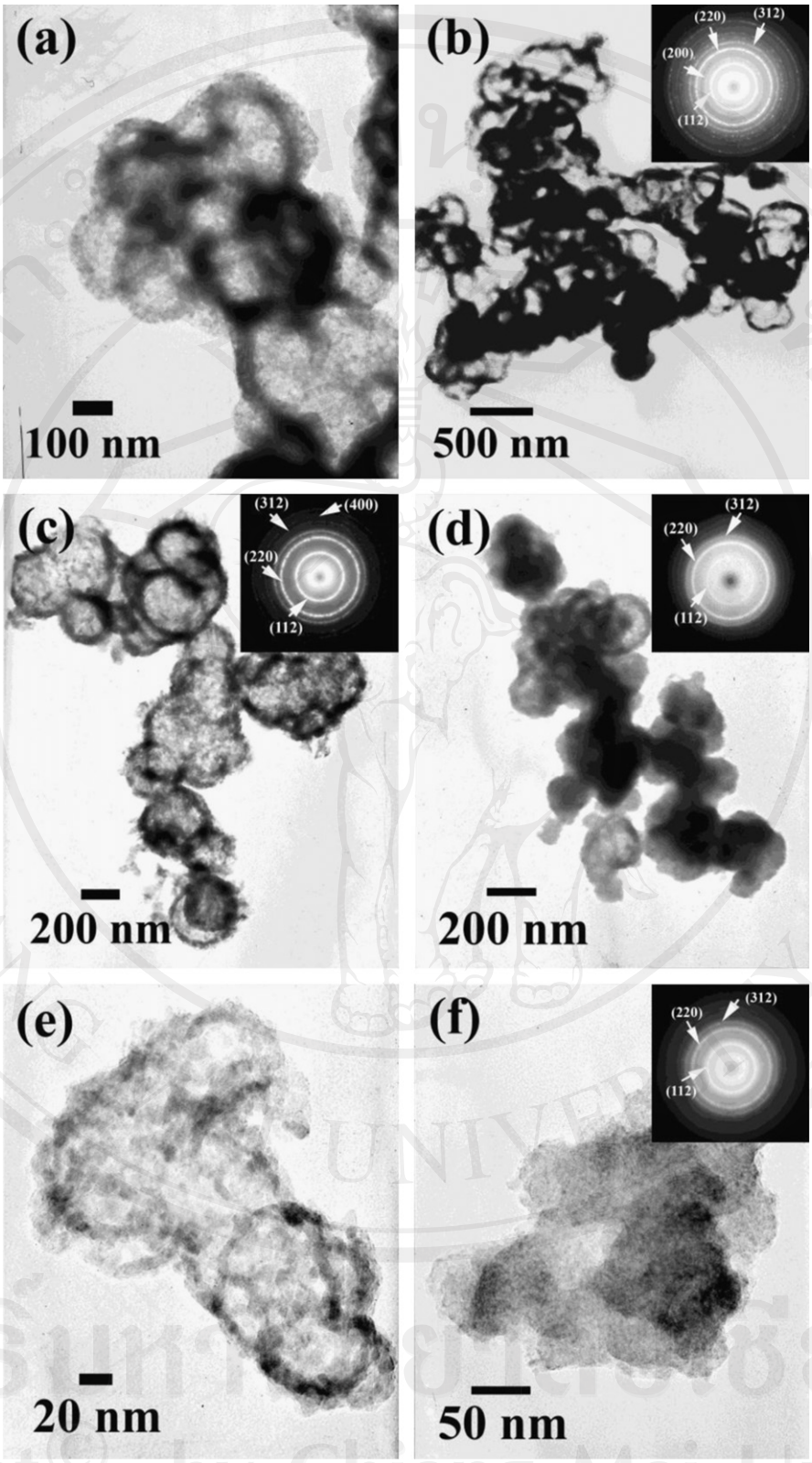

Fig. 3. TEM images and SAED patterns of (a–d) CA-1 synthesized for 40, 40, 20 and 5 cycles, including those of (e,f) CA-2 synthesized for 40 cycles, respectively.

with L-cysteine. During CMR, these complexes were combined and decomposed with the formation of $CuFeS_2$ nuclei. Alternately, [Cu–Fe(L-cysteine) complexes] could form with the subsequent formation of $CuFeS_2$ nuclei.

When $FeCl_2 \cdot 4H_2O$ was used instead of $FeCl_3 \cdot 6H_2O$, $CuFeS_2$ with valence states of Cu^+, Fe^{3+} and S^{2-} was also synthesized. Oxidation–reduction of Fe^{2+} and Cu^{2+} proceeded, including the formation of complexes and $CuFeS_2$ nuclei in sequence as above.

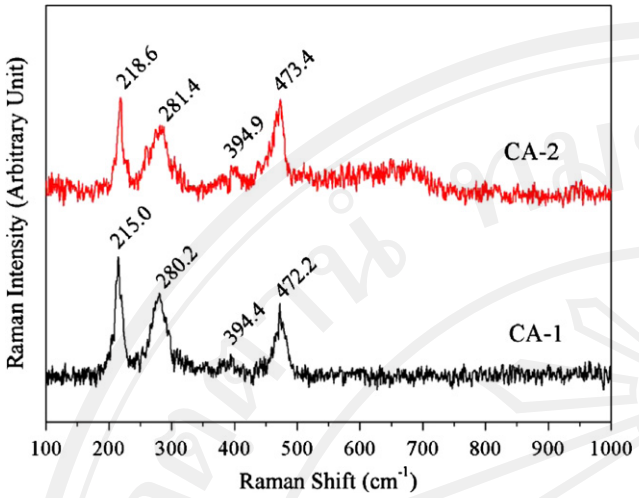

Fig. 4. Raman spectra of CA-1 and CA-2 synthesized for 40 cycles.

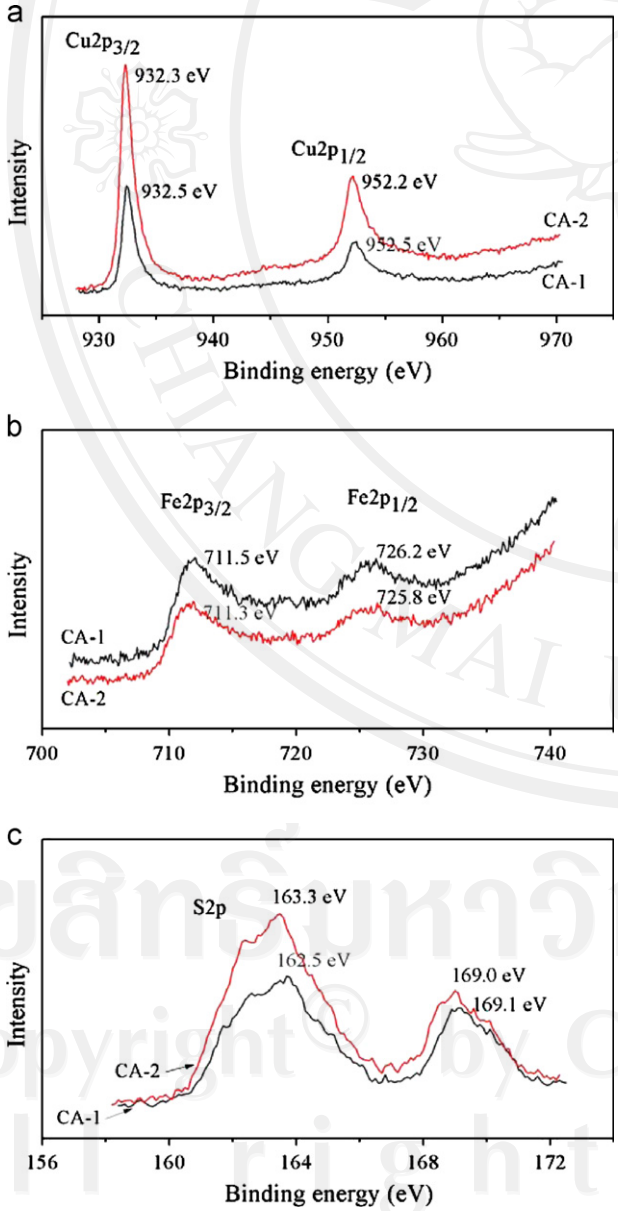

Fig. 5. XPS spectra of (a–c) Cu, Fe and S containing in CA-1 and CA-2 synthesized for 40 cycles, respectively.

The nuclei grew by forming $CuFeS_2$ nanoparticles and clustering in groups with reducing their surface energies.

4. Conclusions

Pure tetragonal $CuFeS_2$ nanoparticles were successfully synthesized by a 300 W CMR, exposing onto EG containing $Cu(CH_3COO)_2$, $FeCl_3 \cdot 6H_2O$ or $FeCl_2 \cdot 4H_2O$ and L-cysteine precursors for 5–40 cycles. Four Raman shifts were detected at 215.0–218.6, 280.2–281.4, 394.4–394.9 and 472.2–473.4 cm^{-1}, and BE of Cu^+ at 932.3–932.5 eV ($Cu2p_{3/2}$) and 952.2–952.5 eV ($Cu2p_{1/2}$), Fe^{3+} at 711.3–711.5 eV ($Fe2p_{3/2}$) and 725.8–726.2 eV ($Fe2p_{1/2}$), and S^{2-} at 162.5–163.3 eV ($S2p_{3/2}$). In this research, Fe-sources played the same role in crystalline degree and size distribution of the products.

Acknowledgments

We wish to thank the Thailand Research Fund for financial support through the research grant BRG5380020 and the Royal Golden Jubilee Ph.D. Program, and the Thailand's Office of the Higher Education Commission through the National Research University Project, including the Graduate School of Chiang Mai University through a general support.

References

[1] Chen KT, Chiang CJ, Ray D. Mater Lett 2013;95:172–4.
[2] Wang MX, Wang LS, Yue GH, Wang X, Yan PX, Peng DL. Mater Chem Phys 2009;115:147–50.
[3] Wang YHA, Bao N, Gupta A. Solid State Sci 2010;12:387–90.
[4] Disale SD, Garje SS. Appl Organomet Chem 2009;23:492–7.
[5] Li J, Tan Q, Li JF. J Alloys Compd 2013;551:143–9.
[6] Ding W, Wang X, Peng H, Hu L. Mater Chem Phys 2013;137:872–6.
[7] Hu J, Lu Q, Deng B, Tang K, Qian Y, Li Y, et al. Inorg Chem Commun 1999;2:569–71.
[8] Powder Diffract File, JCPDS-ICDD. 12 Campus Boulevard, Newtown Square, PA 19073-3273, USA; 2001.
[9] Zhang DE, Xie Q, Wang MY, Zhang XB, Li SZ, Han GQ, et al. Solid State Sci 2010;12:1529–33.
[10] Wang C, Xue S, Hu J, Tang K. Jpn J Appl Phys 2009;48:023003 3pp.
[11] White SN. Chem Geol 2009;259:240–52.
[12] Kuzuya T, Itoh K, Ichidate M, Wakamatsu T, Fukunaka Y, Sumiyama K. Electrochim Acta 2007;53:213–7.
[13] Anzlovar A, Orel ZC, Zigon M. J Nanosci Nanotechnol 2008;8:3516–25.
[14] Ningthoujam RS, Gajbhiye NS, Sharma S. Pramana-J Phys 2009;72:577–86.
[15] Carotenuto G, Pepe GP, Nicolais L. Eur Phys J B 2000;16:11–7.
[16] Orel ZC, Matijević E, Goia DV. J Mater Res 2003;18:1017–22.